Iranian Journal of Oil & Gas Science and Technology, Vol. 11 (2022), No. 3, pp. 37–51
http://ijogst.put.ac.ir

Hydrocarbon Generation Potential and Paleo-Depositional Environments of the Laffan Formation in the Binak Oilfield: Results from Rock-Eval Pyrolysis and Organic Petrographic Studies

Bahram Alizadeh[1], Zollfaghar Eivazi Nejad[2], and Majid Alipour[3*]

[1] Professor, Department of Petroleum Geology and Sedimentary Basins, Faculty of Earth Sciences, Shahid Chamran University of Ahvaz, Ahvaz, Iran
[2] MS Student, Department of Petroleum Geology and Sedimentary Basins, Faculty of Earth Sciences, Shahid Chamran University of Ahvaz, Ahvaz, Iran
[3] Assistant Professor, Department of Petroleum Geology and Sedimentary Basins, Faculty of Earth Sciences, Shahid Chamran University of Ahvaz, Ahvaz, Iran

Highlights

- Rock-Eval pyrolysis results indicate kerogen type II/III in the Laffan formation;
- Organic petrographic studies indicate that inertinites are predominant macerals;
- The presence of bituminite has influenced the Rock-Eval pyrolysis interpretations;
- Pyrolysis data should be combined with organic petrographic observations.

Received: April 9, 2022; *revised*: June 15, 2022; *accepted*: July 19, 2022

Abstract

In this study, the hydrocarbon potential and depositional environments of the Coniacian Laffan formation were investigated in the Binak oilfield, SW Iran. With an average thickness of 80 m, the Laffan formation consists mainly of gray shales and thin argillaceous limestones in the study area. In order to investigate the hydrocarbon potential, 22 cutting samples from 5 wells of the Binak oilfield were analyzed by Rock-Eval 6 pyrolysis and organic petrographic techniques. The hydrogen index (HI) versus T_{max} diagrams indicated mixed-type II/III kerogen with a maturity corresponding to the early stages of the oil window ($T_{max} \approx 435$ °C). In addition, plots of S1+ S2 versus TOC were consistent with a weak to excellent hydrocarbon potential for the Laffan formation. On the other hand, organic petrographic techniques indicated that the primary organic constituents of the Laffan formation are inertinite and bituminite with subordinate amounts of amorphous organic matter (AOM). In other words, the contained organic matter was mainly composed of inertinite and lacked significant hydrocarbon potential. An abundance of inertinite and the conspicuous absence of vitrinite macerals in the studied samples suggested that the Laffan formation was deposited under sub-oxic marine conditions. Furthermore, the presence of bituminite in the studied samples greatly influenced the Rock-Eval pyrolysis readings, so geochemical evaluation of the Laffan formation using only Rock-Eval pyrolysis data may lead to erroneous interpretations. Therefore, a combination of Rock-Eval and organic petrographic methods is necessary for reliable geochemical evaluation of the Laffan formation. The results of this study can be useful for a better understanding of the Cretaceous hydrocarbon system in the study area.

Keywords: Laffan formation, Source rock evaluation, Rock-Eval 6 pyrolysis, Organic petrography, Vitrinite reflectance, Binak Oilfield

[*] Corresponding author:
Email: alipour.magid@gmail.com

How to cite this article
Alizadeh B., Eivazi Nejad Z., and Alipour M., Hydrocarbon Generation Potential and Paleo-Depositional Environments of the Laffan Formation in the Binak Oilfield: Results from Rock-Eval Pyrolysis and Organic Petrographic Studies. Iran J. Oil Gas Sci. Technol., Vol. 11, No. 3, p. 37–51, 2022. DOI: 10.22050/ijogst.2022.336808.1635

1. Introduction

The need to explore new oil resources has led petroleum geologists to pay increasing attention to the issues of hydrocarbon generation, expulsion, migration, and entrapment in the subsurface. The existing source rocks and their maturity should be thoroughly evaluated to better understand the petroleum systems of a sedimentary basin and to reduce the risk of exploration. Hydrocarbon source rocks are fine-grained organic-rich rocks that are capable of generating hydrocarbons (potential source rocks) or have already generated significant amounts of hydrocarbons (effective source rocks) (Peters et al., 2005).

The study area is part of the Zagros Fold-and-Thrust Belt (ZFTB) in the southwest of Iran (southern Dezful Embayment) (Figure 1). The Dezful embayment is located southwest of the Zagros and covers an area of about 40,000 km^2. This area is one of Iran's most important hydrocarbon provinces, with about 45 significant fields (Bordenave, 1995).

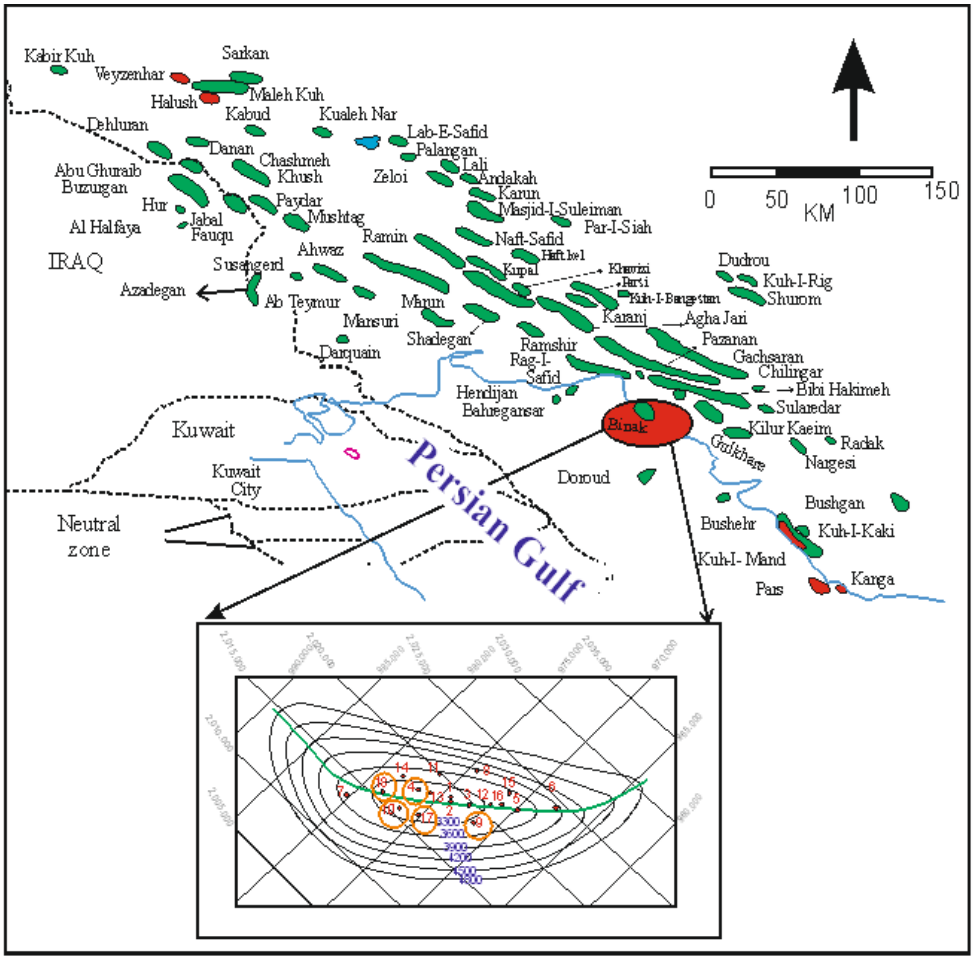

Figure 1

The geographic location of the Binak oilfield in the Zagros basin: the subsurface map at the top of the Sarvak formation and the position of drilled wells (wells used in this study) are shown with orange circles.

The Binak oilfield is located southwest of the Dezful embayment (Figure 1). The presence of oil in this field was proven in 1960 after drilling well number 1, but production started in 1967 after drilling well number 2 (Ansari, 1975). The Laffan formation, with a thickness of about 80 m, has been considered a potential source rock candidate in the Binak oilfield. However, no previous studies have investigated the hydrocarbon generation potential of this formation in detail. Organic geochemical properties of the Laffan formation were mentioned briefly using a limited number of samples (2 samples) based on Rock-Eval pyrolysis data (Fouladvand, 2009). In this study, a systematic sampling from the entire thickness of the Laffan formation is conducted (22 samples). In addition, the Rock-Eval 6 pyrolysis results are combined with organic petrographic observations to gain new insights into hydrocarbon potential and paleo-depositional environments of the Laffan formation. The results of this study are useful for accurate geochemical assessment of the Cretaceous petroleum system and a better understanding of its dynamic evolution in the study area .

2. Geographical location and geology of the study area

The Zagros basin includes the ZFTB, Mesopotamia, and the Persian Gulf (Hooper et al., 1994; Stoneley, 1976). From a structural point of view, the Zagros basin is bounded by the Oman Fault in the southeast, the Anatolian Fault in the northwest, the central Zagros Fault in the northeast, and the Arabian Shield in the southwest (Bahroudi, 2003; Falcon, 1974) (see Figure 2). Regional fault zones intersect the ZFTB, dividing it into various domains from northwest to southeast (e.g., the Lurestan area, the Dezful embayment, and the Fars platform close to the strait of the Hormuz) (Berberian and King, 1981; Takin, 1972) (Figure 2).

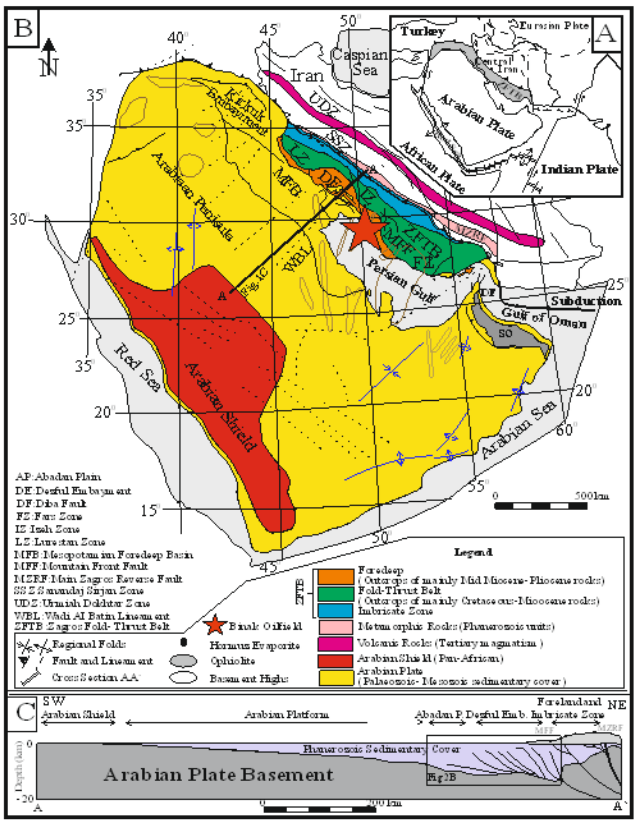

Figure 2

(a) The map showing the Zagros Fold-and-Thrust Belt along the northeast margin of the Arabian Plate, (b) the generalized tectonic map of the Arabian plate and main structural subdivisions of the Zagros basin, and (c) a

simplified cross-section across the Arabian shield, Arabian platform, and the ZFTB along the line A–A′ (AbdollahieFard et al., 2006).

Sedimentary formations in the Binak oilfield generally belong to Cenozoic and Mesozoic systems. The Cenozoic system consists of the Aghajari, Mishan, Gachsaran (i.e., the Fars group), Asmari, and Pabdeh formations, while the Mesozoic system includes the Gurpi formation and other strata belonging to the Bangestan and Khami groups (Figure 3) (Motiei, 1993). In coastal Fars and some parts of the Persian Gulf basin, the Laffan formation acts as an intra-formational seal between the Ilam and Sarvak carbonates (Alipour et al., 2016; Alipour et al., 2019; Alipour et al., 2021). The Laffan shales are lithologically equivalent to the Surgah formation of the Lurestan area in terms of lithology, age, and stratigraphic position. Based on standard stratigraphic definitions in the Persian Gulf basin, these shales are lateral equivalents of the Laffan formation in Qatar (Motiei, 1993). This formation is 84.5 m thick in well 7 of the Binak oilfield and is lithologically composed of gray shales with thin limestone intercalations. However, the thickness decreases to 66 m in well number 6. The upper and lower limits of the Laffan formation are conformable with the Ilam and the Sarvak formations and are usually identified utilizing lithology and gamma-ray logs. Previous biostratigraphic studies have reported a Coniacian age for the Laffan formation (Akbari et al., 2007).

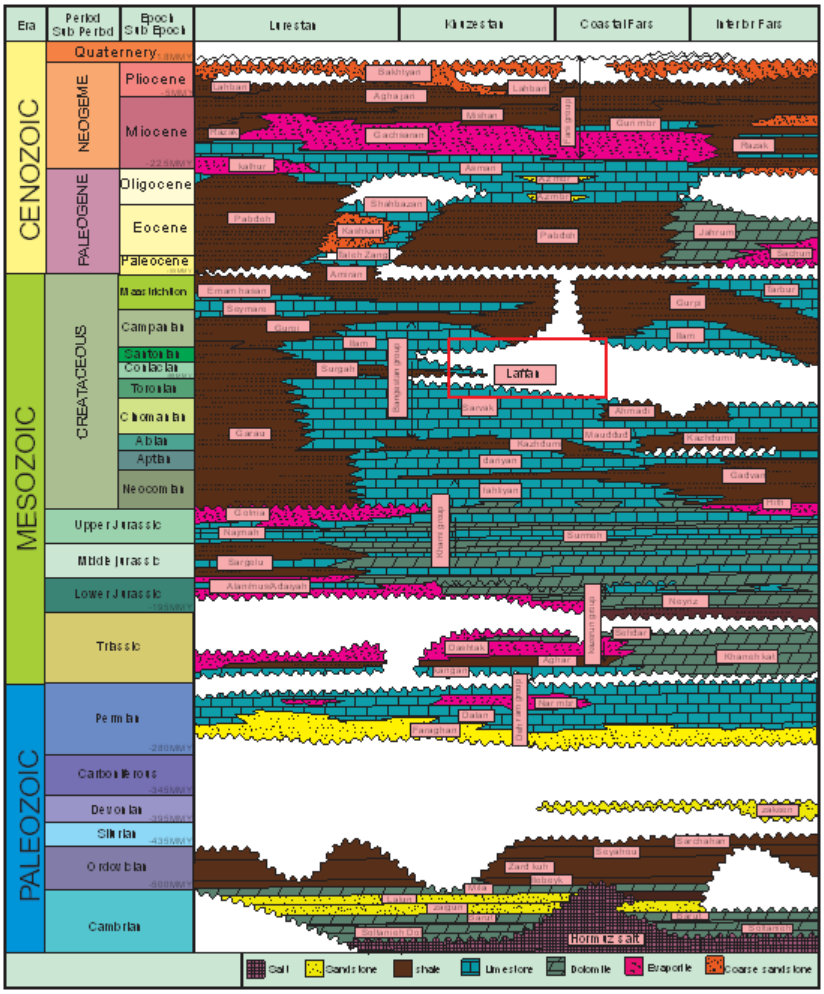

Figure 3

The stratigraphic column of the Zagros from the Cambrian to the Tertiary (Motiei, 1993). The red box shows the studied stratigraphic interval.

3. Methodology

Twenty-two cutting samples from five wells of the Binak oilfield were analyzed by Rock-Eval 6 pyrolysis and organic petrographic techniques to investigate the hydrocarbon potential of the Laffan formation. The analytical procedures and instrumental setup are described in more detail.

3.1. Rock-eval pyrolysis

This study used the Rock-Eval 6 instrument for geochemical evaluation of the 22 cutting samples collected from the Laffan formation (Table 1). After removing contaminants (e.g., drilling additives, mica fragments, iron filings, and hydrocarbon materials), the studied samples were crushed in porcelain mortars. Powdered samples were placed in glass containers and kept inside the oven (25 °C, 24 h) to remove moisture. For Rock-Eval 6 analysis, 50–70 mg of powder samples was carefully loaded into crucibles and analyzed using the standard procedure mentioned in the literature (Espitalié et al., 1977).

Compared to its older versions (e.g., the Rock-Eval II instrument), the Rock-Eval 6 instrument is equipped with more accurate detection systems and applies more precise temperature control over a wide temperature range (Behar et al., 2001). Generally, Rock-Eval pyrolysis provides information on the quantity, quality, and thermal maturity of the organic matter contained in sedimentary rocks (Peters, 1986). This technique uses approximately 70 mg of rock samples to be pulverized and analyzed following standard guidelines (Espitalié et al., 1977). This technique provides information about different fractions of the total organic matter (TOM) in the form of geochemical parameters and calculated ratios (Figure 4) (Lafargue et al., 1998) .

A flame ionization detector (FID) often measures organic compounds released during pyrolysis. The first peak (S1) represents milligrams of free hydrocarbons that can be thermally released from one gram of the rock (Figure 4). The second peak (S2) represents milligrams of hydrocarbons generated by pyrolytic degradation of the kerogen in one gram of the rock (Figure 4). The third peak (S3) represents milligrams of carbon dioxide generated from one gram of rock during temperature programming up to 390 °C and is recorded by a thermal conductivity detector (TCD). The temperature at which the maximum amount of S2 hydrocarbons is generated is called the T_{max} (Figure 4). Other calculated ratios include the hydrogen index (HI), the oxygen index (OI), and the production index (PI). The HI corresponds to the quantity of pyrolyzable organic compounds from the S2 peak relative to the total organic carbon (TOC) of the sample (mg HC/g TOC). The OI measures the quantity of carbon dioxide from the S3 peak relative to the TOC (mg CO_2/g TOC). The PI is defined as the ratio Sl/(Sl+S2) (Figure 4 and Table 1).

Table 1

The Rock-Eval pyrolysis results for the samples of the Laffan formation in the Binak oilfield.

Sample	Well No.	Depth (m)	Lithology	TOC (wt %)	RC	S_1 (mgHC/g rock)	S_2 (mgHC/g rock)	S_3 (mgHC/g rock)	PI	T_{max} ˚C)(	HI (mg HC/g TOC)	OI (mg CO_2/g TOC)
Bk4La1	4	3185	Shale	1.21	0.73	1.86	2.27	2.91	0.45	303	187	240
Bk4La2		3209	Shale	2.87	2.02	1.64	7.73	1.83	0.18	436	269	64
Bk9La1		3281	Shale	0.44	0.29	0.56	0.87	0.92	0.39	419	195	207
Bk9La2		3307	Shale	1.54	1.2	0.48	3.16	1.01	0.13	439	205	65
Bk9La3	9	3311	Shale	12.03	9.6	1.36	26.87	1.65	0.05	429	223	14
Bk9La4		3320	Shale	10.72	8.76	0.98	21.57	1.54	0.04	450	201	14
Bk9La5		3330	Shale	7.84	6.47	0.92	14.65	1.61	0.06	429	187	21

Sample	Well No.	Depth (m)	Lithology	TOC (wt %)	RC	S_1 (mgHC/ g rock)	S_2 (mgHC/ g rock)	S_3 (mgHC/ g rock)	PI	T_{max} °C)(	HI (mg HC/g TOC)	OI (mg CO_2/g TOC)
Bk9La6		3346	Shale	2.74	2.3	0.48	4.28	1.26	0.1	434	156	46
Bk10La1		3160	Shale	1.87	0.75	5.6	7.55	0.77	0.43	434	404	41
Bk10La2		3182	Shale	5.28	2.75	9.61	20.43	1.04	0.32	435	387	20
Bk10La3	10	3204	Shale	4.35	2.75	6.8	11.97	1.05	0.36	429	275	24
Bk10La4		3220	Shale	2.61	1.07	8.37	9.78	0.8	0.46	433	375	31
Bk10La5		3238	Shale	3.35	1.41	7.96	14.98	0.89	0.35	434	447	27
Bk17La1		3162	Shale	1.91	0.98	5.14	5.71	0.99	0.47	427	299	52
Bk17La2		3180	Shale	13.19	9.6	9.69	32.59	1.47	0.23	433	247	11
Bk17La3	17	3200	Shale	7.17	4.95	8.35	17.36	1.76	0.32	434	242	24
Bk17La4		3215	Shale	2.08	1.05	3.58	8.2	1.9	0.3	434	394	91
Bk17La5		3230	Shale	2.7	1.07	8.98	10.11	1.26	0.47	431	375	47
Bk18La1		2986	Shale	0.58	0.39	0.43	1.49	0.95	0.22	432	257	163
Bk18La2	18	3012	Shale	0.71	0.52	0.46	1.16	1.53	0.28	430	165	217
Bk18La3		3030	Shale	1.45	0.65	1.76	6.75	3.02	0.21	442	466	208
Bk18La4		3048	Shale	1.82	0.88	2.77	7.36	3.16	0.27	435	406	174

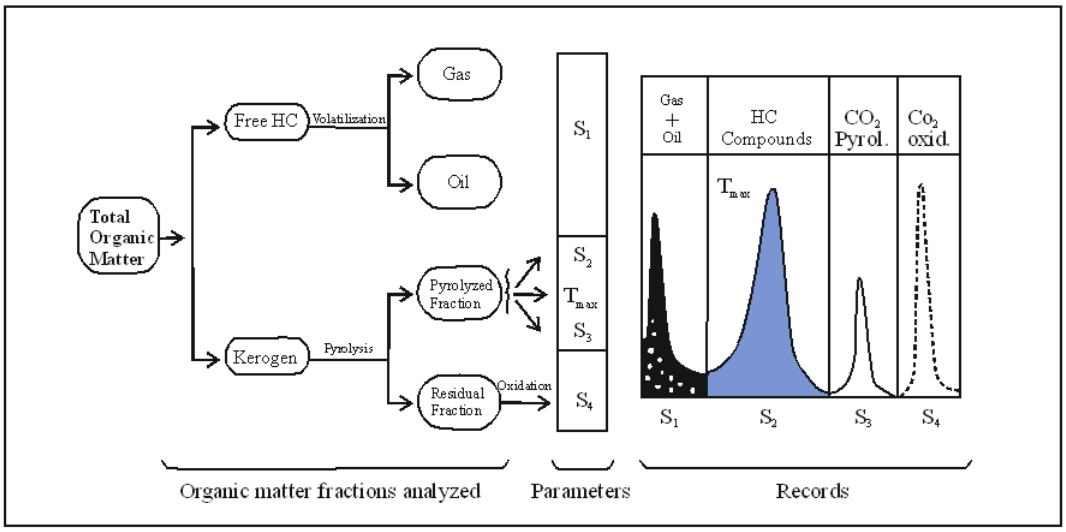

Figure 4

Diagram showing the different fractions of the total organic matter analyzed during the Rock-Eval pyrolysis and the recorded parameters (Lafargue et al., 1998).

3.2. Organic petrography

Organic matter in the sediments can be studied and classified using microscopic techniques by using reflected or fluorescent lights. Microscopic methods provide beneficial information about the quality of the organic matter in sedimentary rocks (Taylor et al., 1998). Macerals are recognizable fragments of sedimentary organic matter whose morphological characteristics are distinguishable under the microscope (Tissot and Welte, 1984; Hunt, 1996). Three main groups of macerals (i.e., liptinites, vitrinites, and inertinites) are identified in sedimentary rocks (Stach et al., 1982).

Liptinite or exinite consists mainly of the algae, pollen, spores, and cuticles of the plant; fats; and plant oil (Stach et al., 1982; Taylor et al., 1998). In 1964, it was suggested that the term liptinite be used instead of exinite (Stach et al., 1982). Liptinitic macerals are usually not present in high concentrations in sedimentary rocks and are usually found in playa lakes and shallow swamps (Stach et al., 1982). These macerals are mostly oil-prone and have low reflectance and high fluorescence at low maturity (Taylor et al., 1998). Liptinite phytoclasts are composed of very different origins and have specific shapes and unique textures, such as Tasmanite algae, resin, spores, and pollen (Stach et al., 1982; Hunt, 1996).

Vitrinite is a woody maceral derived from terrestrial higher plants (Stach et al., 1982). This maceral has appeared in the sedimentary record since the Devonian due to the spread of continental higher plants and often has angular shapes (Taylor et al., 1998). They have a cellular structure and are primarily gas-prone (Hunt, 1996). This maceral is one of the essential and abundant maceral groups in bituminous coals, but it is less abundant in shales and occurs in small dimensions (Stach et al., 1982; Mukhopadhyay and Dow, 1994). The vitrinite group is subdivided into telinite, collinite, and vitrodetrinite groups (ICCP, 1998).

Inertinite macerals have no potential for hydrocarbon generation and include angular shapes with distinct cellular structures (Scott and Glasspool, 2007). These macerals do not have fluorescence properties and are distinguished from others in reflected light by having a high reflectivity and dull color (Taylor et al., 1998; Peters et al., 2005). The origin of inertinites varies and is associated with severe oxidation before deposition. Inertinites are usually abundant where previously deposited organic matter undergoes another sedimentation cycle (Stach et al., 1982; Scott and Glasspool, 2007; Taylor et al., 1998).

In this study, all the available samples were examined by organic petrographic techniques (i.e., 22 samples from 5 different wells) (see Table 1). To this end, the cutting sample of the source rock is placed inside the epoxy resin adhesive and carefully polished, following standard guidelines for sample preparation (Figure 5) (ASTM, 2014; Stach et al., 1982). Microscopic studies of samples were performed using an advanced Zeiss Axioplane (II) microscope equipped with a J&M photomultiplier located at the petroleum geology laboratory of the Shahid Chamran University of Ahvaz .

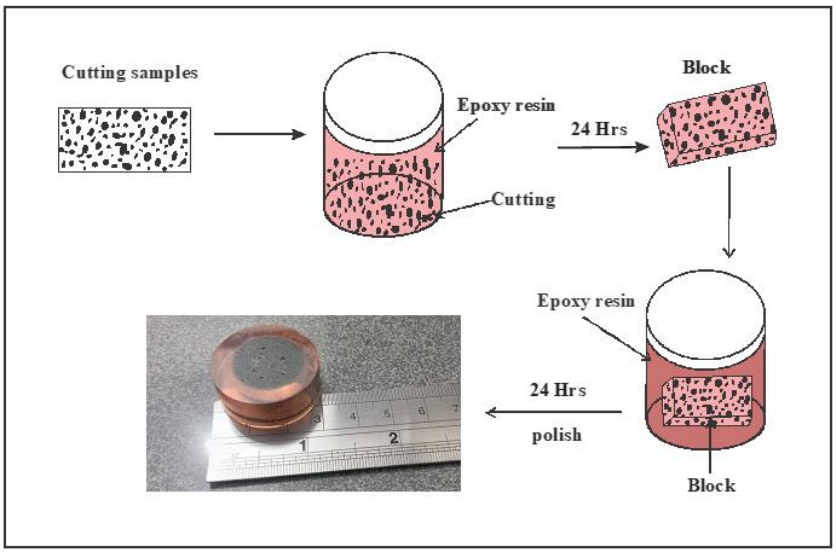

Figure 5

Schematics of the steps for preparing polished pellets for organic petrographic studies. Cutting chips of the source rock are placed inside the epoxy resin adhesive and carefully polished, following standard guidelines.

4. Results and discussion

4.1. Rock-eval pyrolysis results

The results of the Rock-Eval pyrolysis of 22 samples from the Laffan formation in the Binak oilfield are presented in this study (Table 1). A quick look at the parameters in Table 1 indicates that anomalously higher S1 readings characterize some samples. Considering the low maturity of the analyzed samples (i.e., T_{max} readings in Table 1), these high S1 readings were considered a sign of non-indigenous free hydrocarbons in the rock matrix. This finding is also supported by the general shape of the Rock-Eval pyrographs obtained for these samples (Figure 6). In addition, some samples are characterized by higher OI readings, which can result from the organic matter oxidation during the deposition in the sedimentary environment (see Table 1) .

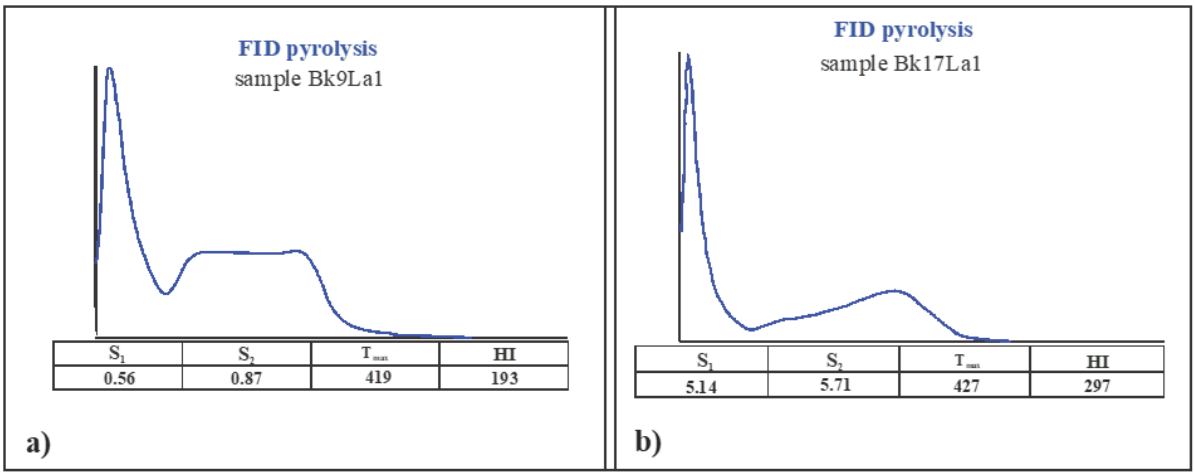

Figure 6

Rock-Eval pyrographs obtained for samples (a) Bk9La1 and (b) Bk17La1 of the Laffan formation in the Binak oilfield (see Table 1).

Diagrams of S1 versus TOC are used to ensure that the studied samples are not contaminated (Figure 7a). Based on these diagrams, some samples are plotted above the line and are characterized by anomalously higher S1 readings, as discussed above .

The hydrocarbon generation potential of the Laffan formation was evaluated in this study using diagrams of S1+S2 versus TOC (Figure 7b). Based on this diagram, the Laffan formation has weak to excellent hydrocarbon potential in the Binak oilfield (Figure 7b). Nevertheless, based on the classification of source rocks in terms of the total organic carbon content (e.g., Peters et al., 2005), the Laffan formation can be classified as a “good” to a “very good” source rock.

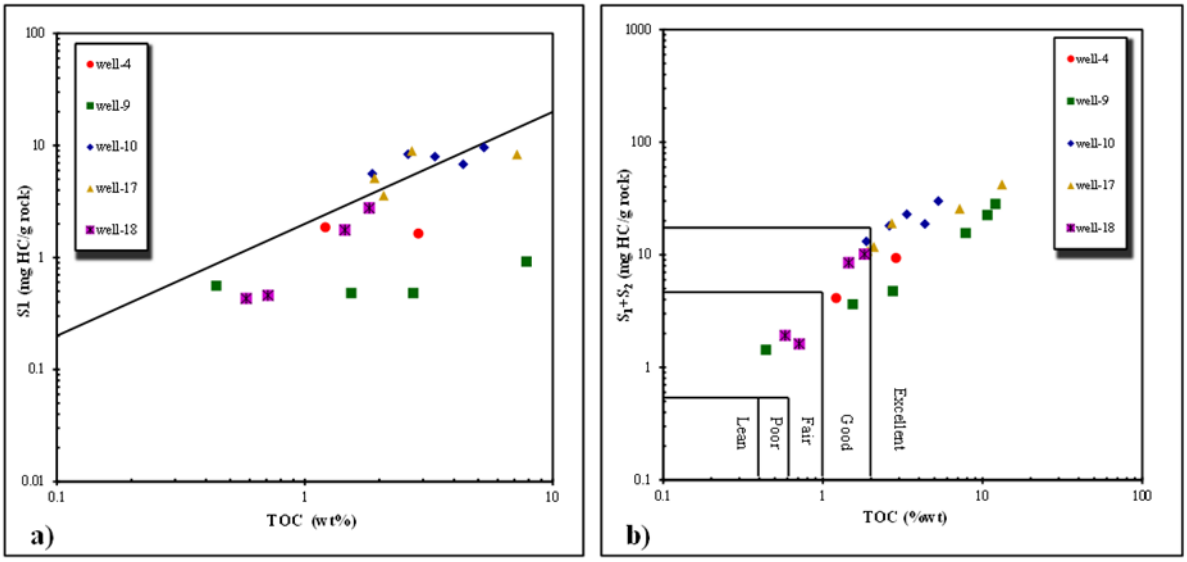

Figure 7

(a) S1 versus TOC diagram indicating the presence of free hydrocarbons (modified after Hunt, 1996), and (b) S1+S2 versus TOC diagram to evaluate the hydrocarbon generation potential of the Laffan formation in the Binak oilfield (modified after Huang et al., 1999).

This study used the diagrams of the HI versus the OI to define the kerogen type existing in the Laffan formation (Figure 8a). These diagrams suggest that the studied samples contain a mixture of type II and III kerogens, confirmed by the HI versus T_{max} plots (Figure 8b). In addition, the plots of HI versus T_{max} for our studied samples indicated that the Laffan formation contained organic matter in the early stages of oil generation ($T_{max} \approx 435$ ˚C) (Figure 8b) .

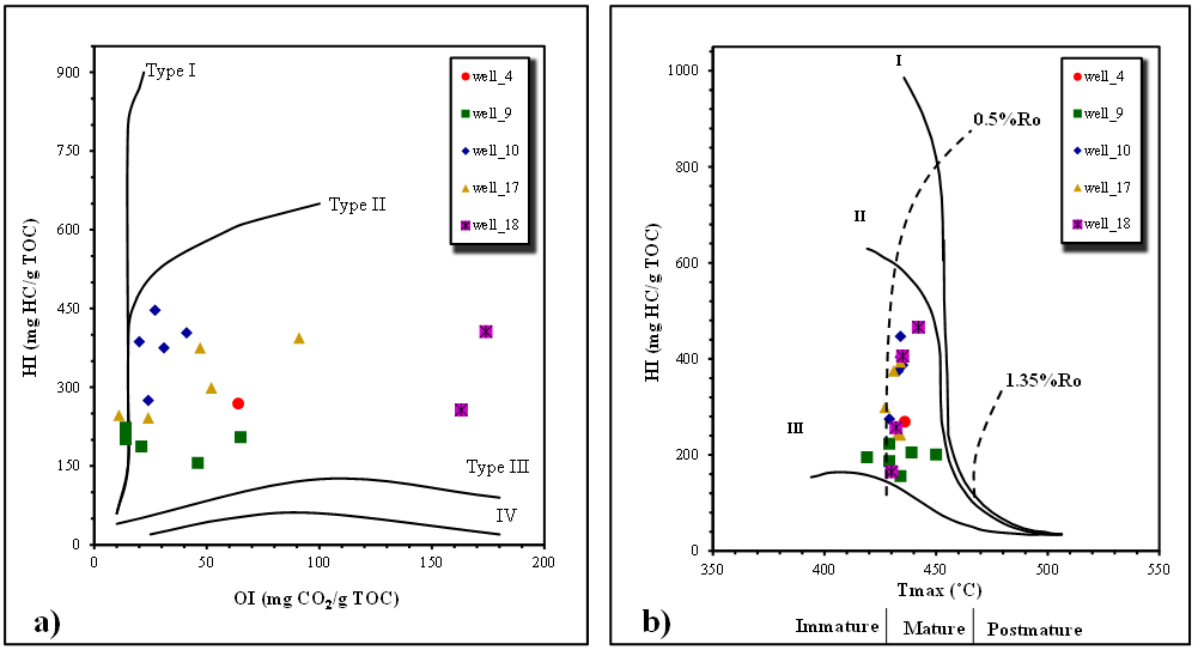

Figure 8

(a) The HI versus the OI diagram indicating the type of organic matter, and (b) the HI versus T_{max} diagram showing the thermal maturity of the studied samples from the Laffan formation in the Binak oilfield (modified after Hunt, 1996).

4.2. Organic petrographic results

After examining the Laffan formation in the studied wells by Rock-Eval 6 pyrolysis technique, petrographic studies were conducted to better evaluate the contained organic matter. Generally, organic petrographic studies under reflected white light indicated that fusinite, bituminite, semifusinite, inertodetrinite, and amorphous organic matter (AOM) existed in various proportions in the studied samples. Nevertheless, the main components of organic matter in the Laffan formation were inertinite, bituminite, and a small amount of amorphous organic matter (Figures 9–11).

The co-occurrence of liptinites and inertinites in the studied samples suggested that organic matter in the Laffan formation should be a mixture of type II and III kerogens. This aligns with results obtained from the Rock-Eval pyrolysis of the studied samples (Figure 8a and 8b).

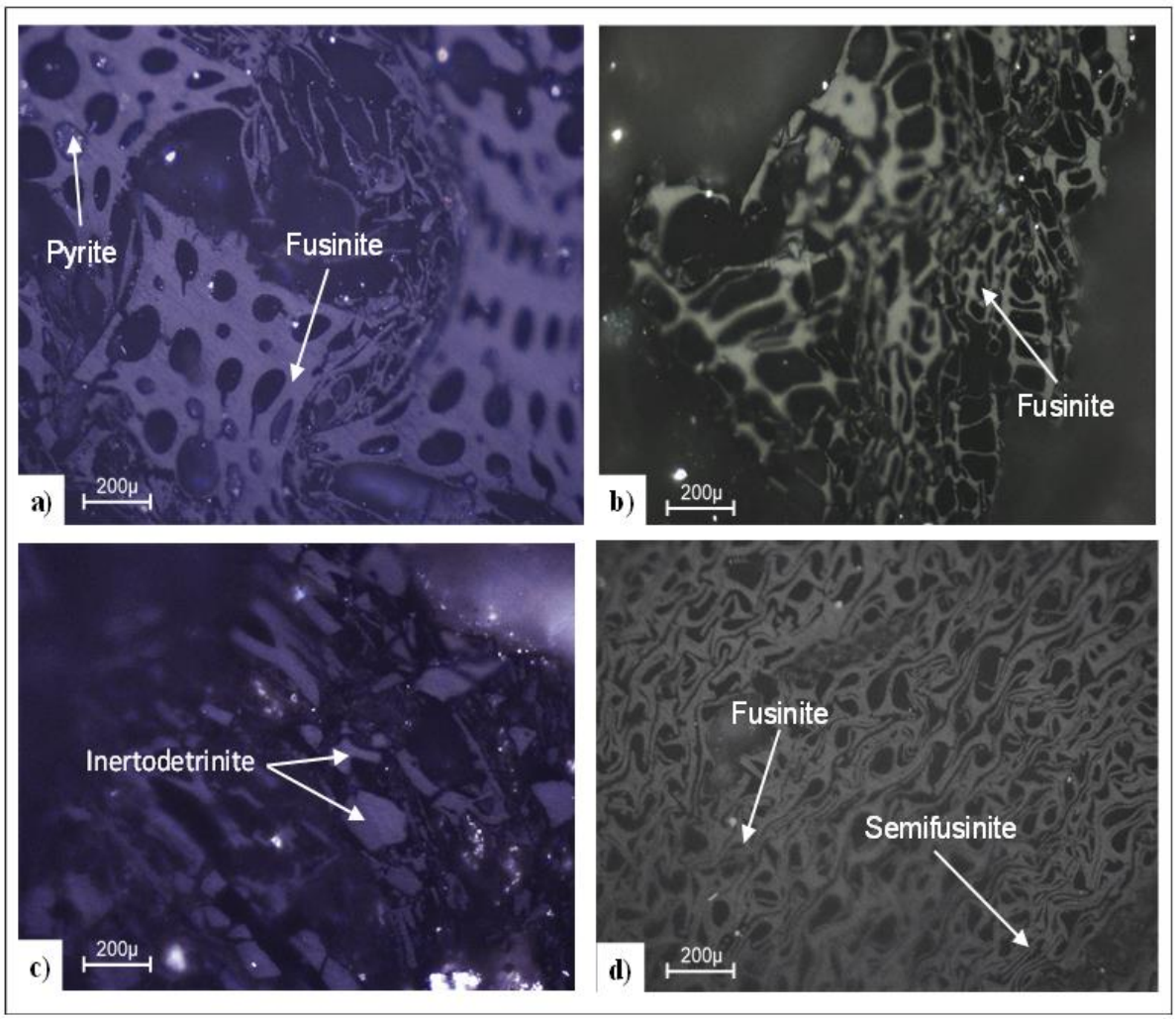

Figure 9

Examples of organic petrographic photomicrographs from the Laffan formation in the Binak oilfield (Sample Bk17La3, Table 1) indicating fusinite with a sieve structure with cavities filled by (a,b) pyrite, (c) inertodetrinite, and (d) semifusinite and fusinite.

Notably, the presence of bituminite in the studied samples could have influenced the results of Rock-Eval pyrolysis. Thus, geochemical assessment of the Laffan formation based only on the Rock-Eval pyrolysis results may lead to erroneous interpretation. Therefore, in this study, the geochemical evaluation of the Laffan formation was conducted by combining organic petrographic and Rock-Eval

pyrolysis results. Accordingly, it is concluded that the organic matter in the Laffan formation is composed mainly of inertinite and bituminite (Figures 10 and 11) and has negligible hydrocarbon generation potential. According to the organic petrographic results, the absence of vitrinite macerals in the studied formation and a conspicuous abundance of inertinites confirms that the Laffan formation is deposited under oxic marine conditions (Figure 11).

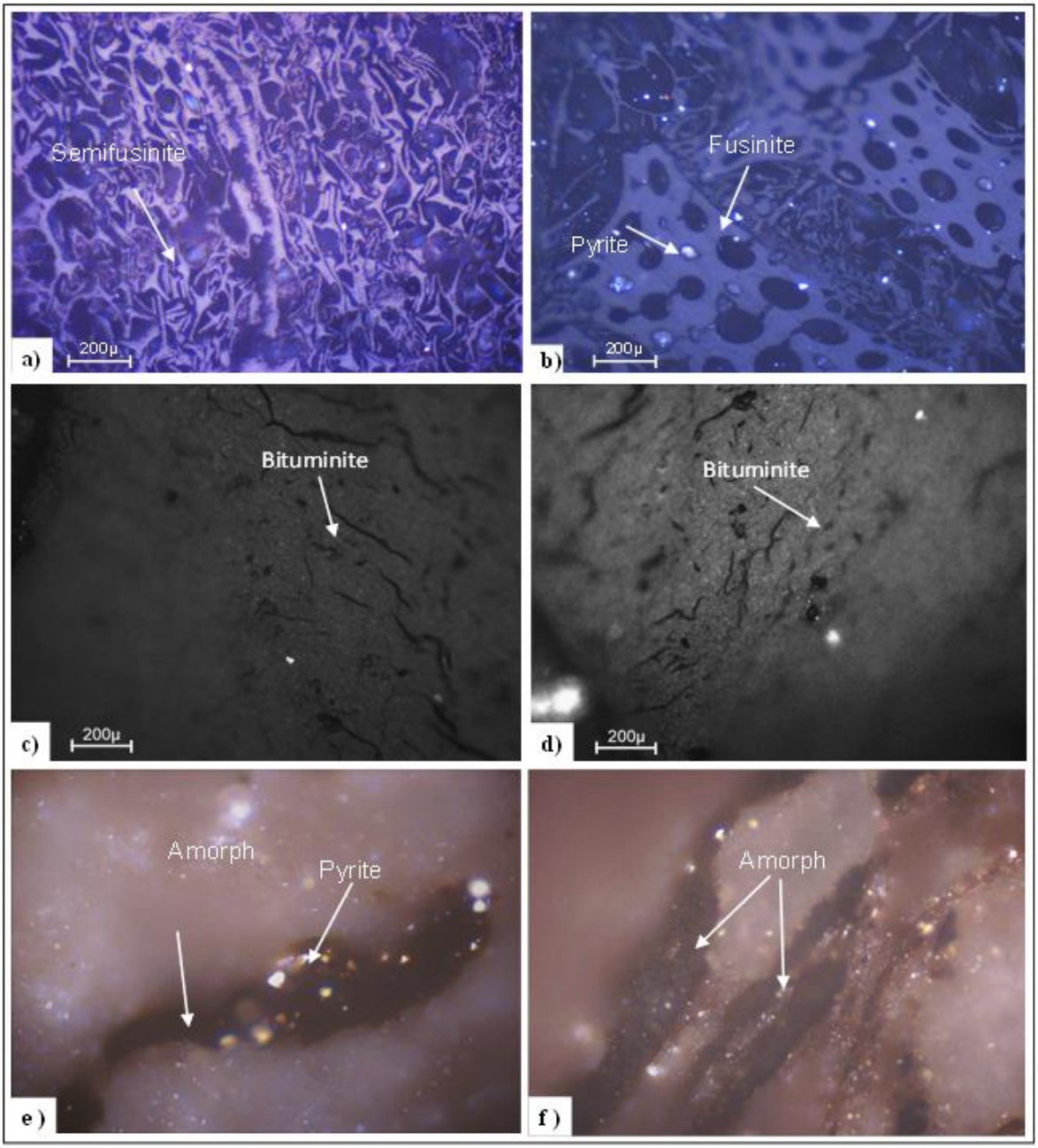

Figure 10

Examples of organic petrographic photomicrographs from the Laffan formation in the Binak oilfield (Sample Bk18La3, Table 1) indicating (a) semifusinite, (b) fusinite with a sieve structure with cavities filled by pyrite, (c,d) high reflectance bituminite, and (e,f) amorphous organic matter in the form of thin veins replaced by pyrite.

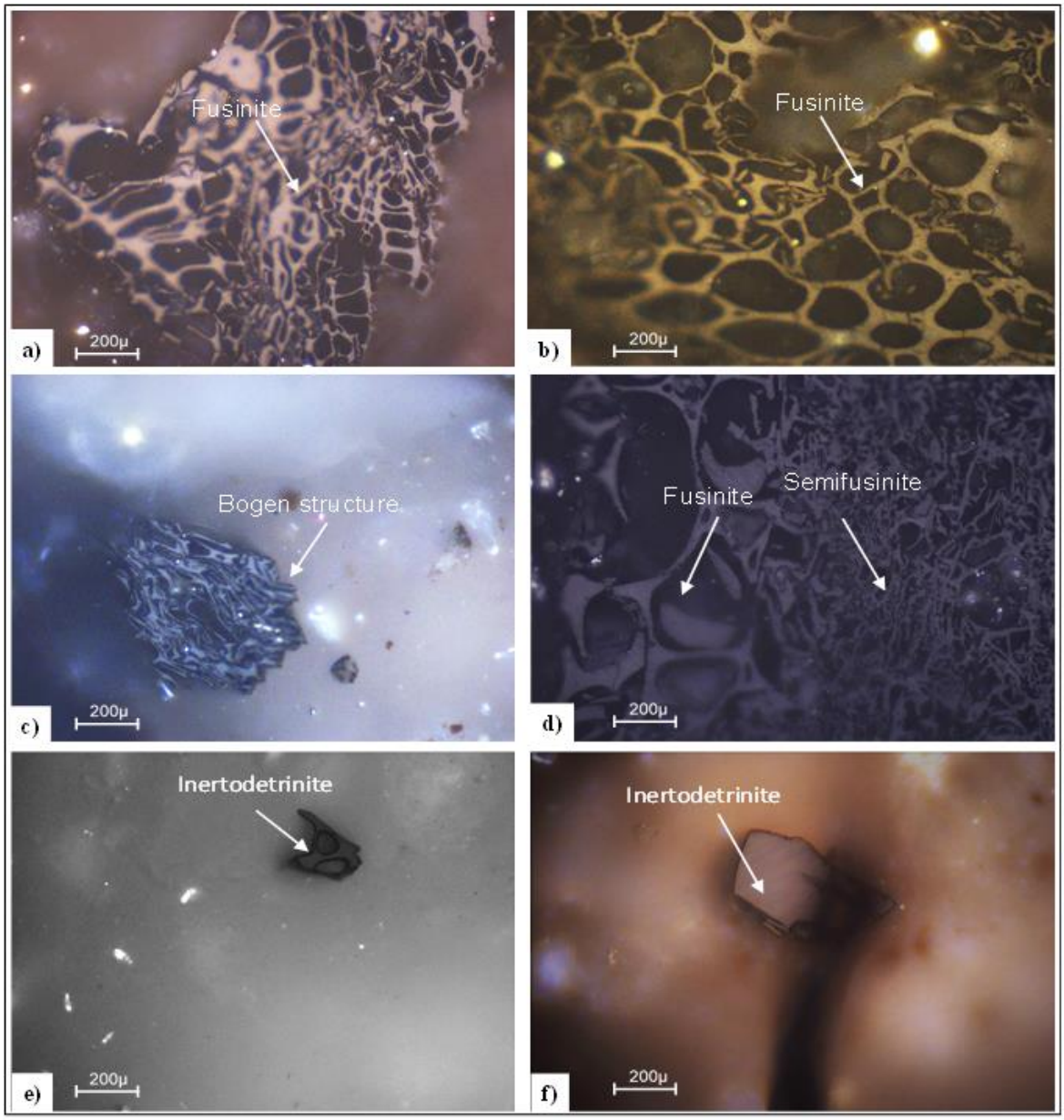

Figure 11

Photomicrographs of Sample Bk9La4 from the Laffan formation in the Binak oilfield, indicating (a,b) fusinite, (c) Bogen structures formed as a result of breaking of the empty cell wall of the fusinites, (d) semifusinite and fusinite, and (e,f) inertodetrinite.

5. Conclusions

Based on the results of Rock-Eval 6 pyrolysis (i.e., the HI versus T_{max} diagrams), the kerogen type of the Laffan formation in the Binak oilfield is a mixture of type II and III kerogens. In addition, the plots of the HI versus T_{max} indicated that the studied samples had reached the early stages of oil generation ($T_{max} \approx 435$ °C). Plots of S1+S2 versus TOC suggested weak to excellent hydrocarbon potential for the Laffan formation. However, organic petrographic techniques showed that the organic matter in this formation mainly comprised inertinite and bituminite, along with subordinate amounts of amorphous organic matter. Notably, the bituminite in the studied samples could have impacted the Rock-Eval pyrolysis results. Thus, Rock-Eval pyrolysis data alone might not provide a reliable assessment of the

organic geochemical properties of the Laffan formation. Accordingly, combining organic petrographic results with Rock-Eval pyrolysis data provided an alternative means for the geochemical assessment of the studied samples. This multi-disciplinary approach conclusively suggested that the organic matter in the Laffan formation was of type II/III origin, deposited under sub-oxic marine conditions, with negligible hydrocarbon potential. Our findings suggested that the Laffan formation should not be an influential rock source in the Cretaceous petroleum system. Therefore, further studies are required to investigate its role as an intra-formational seal rock, which can influence hydrocarbon migration and entrapment in the Sarvak and Ilam limestones in the study area.

References

Abdollahiefard, I., Braathen, A., Mokhtari, M., and Alavi, S. A., Interaction of The Zagros Fold–thrust Belt and The Arabian-type, Deep-Seated Folds in The Abadan Plain and The Dezful Embayment, SW Iran: Petroleum Geoscience, Vol. 12, No. 4, p. 347–362, 2006.

Akbari et al., Study of Microfacies, Sedimentary Environment, Stratigraphic and Biostratigraphic Sequence of The Bangestan Reservoir in The Binak Oilfield, Report No. 6187 P., Deputy Director - Expansion Geology, Basic Geology Department, 2007.

Alipour, M., Alizadeh, B., Chehrazi, A., Mirshahani, M., and Khani, B., Sequence Stratigraphic Control on Active Petroleum System in The Eastern Block A, Persian Gulf, The 1st International Conference on Science and Basic Research: Kharazmi Higher Institute of Science and Technology, Iran, p. 151–153, 2016.

Alipour, M., Alizadeh, B., Chehrazi, A., and Mirzaie, S., Combining Biodegradation in 2D Petroleum System Models: Application to The Cretaceous Petroleum System of The Southern Persian Gulf Basin: Journal of Petroleum Exploration and Production Technology Vol. 9, p. 2477–2486, 2019.

Alipour, M., Alizadeh, B., Mirzaei, S., and Chehrazi, A., Basin and Petroleum System Analysis in The Southeastern Persian Gulf Basin: A 2D Basin Modeling Approach: Journal of Petroleum Exploration and Production Technology, Vol. 11, No. 12, p. 4201–4214, 2021.

Ansari, A. A. S., N. H., The Binak Field Reservoir Study Asmari and Bangestan. Report No. 2724 P., Reservoir Geology and Reservoir Engineering Studies Departments, Oil Service Company of Iran, Ahwaz, 1975.

ASTM, ASTM D7708-14, Standard Test Method for Microscopical Determination of The Reflectance Of Vitrinite Dispersed in Sedimentary Rocks: West Conshohocken, PA, 2014.

Bahroudi, A., The Effect of Mechanical Characteristics of Basal Decollement and Basement Structures on Deformation of The Zagros Basin: Uppsala University Library, 2003.

Behar, F., Beaumont, V., and Penteado, H. D. B., Rock-Eval 6 Technology: Performances and Developments: Oil & Gas Science and Technology, V. 56, No. 2, p. 111–134, 2001.

Berberian, M., and King, G., Towards A Paleogeography and Tectonic Evolution of Iran: Reply: Canadian Journal of Earth Sciences, Vol. 18, No. 11, p. 1764–1766, 1981.

Bordenave, M., and Huc, A., The Cretaceous Source Rocks in The Zagros Foothills of Iran: Revue De L'institut Français Du Petrole, Vol. 50, No. 6, p. 727–752, 1995.

Espitalié, J., Madec, M., Tissot, B., Mennig, J., and Leplat, P., Source Rock Characterization Method for Petroleum Exploration, in Proceedings Offshore Technology Conference Onepetro, 1977.

Falcon, N. L., Southern Iran: Zagros Mountains: Geological Society, London, Special Publications, Vol. 4, No. 1, p. 199–211, 1974,

Fouladvand, R., Burial History Reconstruction and Evaluation of Thermal Maturity and Hydrocarbon Generation in Binak Oilfield. MS Thesis, Shahid Chamran University of Ahvaz, 157 P., 2009.

Hooper, R., Baron, I., Agah, S., Hatcher, R., and Al-Husseini, M., The Cenomanian to Recent Development of The Southern Tethyan Margin in Iran: Middle East Petroleum Geosciences GEO, Vol. 2, p. 505–516, 1994.

Huang, D., Liu, B., Wang, T., Xu, Y., Chen, S., and Zhao, M., Genetic Type and Maturity of Lower Paleozoic Marine Hydrocarbon Gases in The Eastern Tarim Basin: Chemical Geology, Vol. 162, No. 1, p. 65–77, 1999.

Hunt, J., Petroleum Geochemistry and Geology, WH Freeman and Co, San Francisco, 743 P., 1996.

ICCP, The New Vitrinite Classification (ICCP System 1994): Fuel, Vol. 77, No. 5, p. 349–358, 1998.

Lafargue, E., Marquis, F., and Pillot, D., Rock-Eval 6 Applications in Hydrocarbon Exploration, Production, and Soil Contamination Studies: Revue De L'institut Français Du Pétrole, Vol. 53, No. 4, p. 421–437, 1998.

Motiei, H., Stratigraphy of The Persian Gulf, 590 P, 1993.

Mukhopadhyay, P. K., and Dow, W. G., Vitrinite Reflectance as A Maturity Parameter: Applications and Limitations, American Chemical Society, 1994.

Peters, K. E., Guidelines for Evaluating Petroleum Source Rock Using Programmed Pyrolysis: AAPG Bulletin, V. 70, No. 3, p. 318–329, 1986.

Peters, K. E., Peters, K. E., Walters, C. C., and Moldowan, J.,The Biomarker Guide, Cambridge University Press, 1155 P, 2005.

Scott, A. C., and Glasspool, I. J., Observations and Experiments on The Origin and Formation of Inertinite Group Macerals: International Journal of Coal Geology, Vol. 70, No. 1–3, p. 53–66**.** 2007.

Stach, E., Mackowsky, M. T., Teichmuller, M., Taylor, G., Chandra, D., and Teichmuller, R., Stach's Textbook of Coal Petrology, Berlin, Gebruder, Borntraeger, 535 P., 1982.

Stoneley, R., On the Origin of Ophiolite Complexes in The Southern Tethys Region: Reply: Tectonophysics, Vol. 34, No. 3–4, p. 262–265, 1976.

Takin, M., Iranian Geology and Continental Drift in The Middle East: Nature, Vol. 235, No. 5334, p. 147–150, 1972.

Taylor, G. H., Teichmüller, M., Davis, A., Diessel, C., Littke, R., and Robert, P., Organic Petrology**.** 1998.

Tissot, P. and Welte, D., Petroleum Formation and Occurrence, Springer, 529 P., 1984.

This article is an open-access article distributed under the terms and conditions of the Creative Commons Attribution 4.0 International (CC BY 4.0) (https://creativecommons.org/licenses/by/4.0/)